RESONANT ULTRASOUND SPECTROSCOPY FOR ANALYSES THE INFLUENCE OF SPECIAL ALLOYS CONSTITUTIVE ELEMENTS ON MECHANICAL PROPERTIES

Adriana Savin[1*], Mihail-Liviu Craus[1,2], Rozina Steigmann[1], Vitalii Turchenko[2]

[1] Nondestructive Testing Department, National Institute for R&D for Technical Physics, Iasi, Romania; asavin@phys-iasi.ro

[2] Frank Laboratory for Neutron Physics, Joint Institute for Nuclear Research, Dubna, Russia,

Abstract: The Ni-Mn-Ga alloy family is extreme sensitivity to the variation of the Ga component in the structure as well as under the action of a low stress. A major bottleneck in using Ni-Mn-Ga FSMA is their extreme fragility, which has been attributed to the reduced strength at the border of the grains. The microstructure combined with the high mechanical anisotropy make these alloys susceptible to intergranular fracture. The analysis of the elastic constants in the entire sample volume using the RUS method allows a qualitative investigation correlated with the crystallographic properties at micro / macroscopic level.
Keywords: Alloys, resonant frequency, resonant ultrasound spectroscopy, mechanical parameters

1. INTRODUCTION

For centuries, materials have played an important role as structural materials. New technologies for making electronic devices and circuits involve the use of new materials, which consist of composite structures made based on the special properties of the components. Heusler alloys, represent a class of smart materials, that have received a lot of attention in the past few years [1].The path to new applications of these materials required their characterization, the determination and optimization of working parameters, the analysis of new phenomena and material effects as well as the determination of the interaction between the constituent elements. Over time, Heusler alloys as multifunctional materials have found applications such as conventional shape memory effect [2], half-metallicity [3], and later those related to properties induced by the application of a magnetic field. Some of magnetic-field-induced strain (FSMAs) can be used in spintronic devices (with advantages and disadvantages)[4], actuators and shape memory. Two families of Heusler type alloys are known, half Heusler with the generic formula XYZ, which crystallizes in a non-centrosymmetric cubic structure (SG $F\bar{4}3m$) and in cubic structure (SG $Fm\bar{3}m$). For the alloy X_2YZ, the two atoms occupying the tetrahedral X positions make possible the magnetic interaction between the X atoms and a secondary magnetic sub lattice [5].

Heusler alloys are mostly ferromagnetic that saturates in the outer field less than 0.5T at low temperature, but can also be antiferomagnetic especially in those alloys in which the Y position is occupied by Mn. Generally, he well-known example of Ni−Mn-based these alloys have exotic properties [6], such as colossal magnetostriction, potential inverse magnetocaloric effect (MCE) and large magnetoresistance output. These functional properties strongly depend on the field-driven magneto-structural transitions with variations of magnetic behavior and microstructures. The structure of Ni−Mn Heusler alloys are a high temperature $L2_1$ type structure (SG $Fm\bar{3}m$) or B2 austenite type structure (SG $Pm\bar{3}m$)[7]. The $L2_1$ austenite displays strong ferromagnetism below its Curie point T_c, while under martensite transition point Ni_2MnX Heusler alloys behave as paramagnetic, antiferromagnetic, ferromagnetic and spin-glass phases. The FSMAs prototype is represented by Ni_2MnGa which has a field deformation effect up to 1T but also Ni_2MnZ (Z = Al, Co) has the most familiar type [8]. For Ni_2MnZ (Z = Ga, Al) these Heusler alloys have special magneto-mechanical properties, such as magnetic shape memory effect and magnetic field-induced superelasticity, properties that make them attractive for information storage sensors [5]. However, studies do not recommend Ni_2MnGa for magneto-mechanical devices due to the fragility and low temperature at which the martensitic transition takes place [9]. The family of Ni-Mn-Ga alloys present large strain [10] in magnetic field due to the double delimitation movement in the martensitic phase.

The objectives of this work were to obtain the essential thermal properties during the transition of the ferromagnetic state to paramagnetic state at temperature higher as room temperature (T_r) and the possibility to correlate of the elastic parameters and of the frequency obtained of RUS with the crystallographic structure of the sample. The analysis of the elastic constants in the entire sample volume using the RUS method allows a qualitative investigation correlated with the crystallographic properties.

2. MATERIALS AND METHODS

Heusler alloys are possible candidates for magnetic shape memory (MSM) alloys, due its high Curie and martensitic/austenitic transformation temperature. The B2 crystallographic state has been reported as antiferromagnetic or spin-glass, while the $L2_1$ phase is associated with the ferromagnetic state. The ($Ni_{50}Mn_{25}Ga_{25}$ – NMG and $Ni_{50}Mn_25Ga_{12.5}Al_{12.5}$ – NMAG) alloys analyzed, was prepared by standard arc melting technique of the constituent elements, the phase composition, the lattice type and the unit cell constants were also determined according to [11]. Direct measurement of the elastic constants of Ni-Mn-Ga FSMA does not reveal a large effect of the field on the constants. The strong elastic anisotropy of the austenitic phase makes the observation and calculation relatively ambiguous, differing significantly. A major bottleneck in using Ni-Mn-Ga FSMA is their extreme fragility, which has been attributed to the reduced strength at the border of the grains. The microstructure combined with the high mechanical anisotropy make these alloys susceptible to intergranular fracture. The analysis of the elastic constants in the entire sample volume using the RUS method allows a qualitative investigation correlated with the crystallographic properties at micro / macroscopic level. This would emphasize the orientation of grains in austenitic Ni-Mn-Ga for SMA structural applications.

For calculated mechanical parameter was used ultrasound method by echo pulse method, described in [12] in order to determine Young modulus E, shear modulus G and Poisson ratio of sample using longitudinal velocity wave C_l and transversal velocity wave C_t presented in table 1. The average values of hardness were obtained from five different areas of faces of sample remains approximately constant. The small differences are due to the influence of alloying elements that influence compactness.

Table 1: Sample characteristics

sample	S [mm²]	h [mm]	Density [g/mm³]	E [GPa]	G [GPa]	ν	C_l [m/s]	C_t [m/s]
NMG	55.38	8.7	5841	109	32	0.38	5185	2352
NMAG	58.05	8.4	5664	118	45	0.32	5352	2835

In most cases for Heusler compounds only the magnetic properties related to the structure are analyzed in theory-experiment comparisons [13], but the need for structural applications proves that physical parameters obtained by calculations and experiment (vibrational, mechanical properties) are equally important.

Resonant ultrasound spectroscopy (RUS) can in principle be applied to materials with well-defined geometric shapes regardless of crystallographic symmetry. Traditionally, the elastic constants required for simulations to calculate resonant frequencies are derived from measurements of elastic wave propagation velocities [14].

Figure 1 shows the flow of information received from the combination of methods used in determining the elasticity properties for millimeter-sized samples; mechanical testing methods, in which the elastic properties are obtained from the stress-strain relationship in low frequency mode and the ultrasound method in which the propagation speed is directly related to the elastic constants[15].
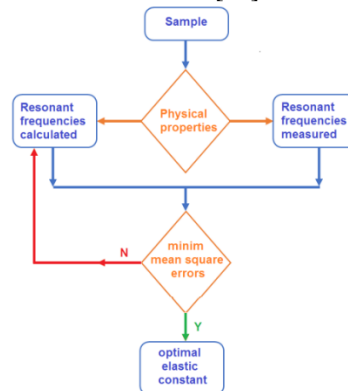
Figure 1: Principle of elastic properties determination

RUS has the ability to make mechanical resonance measurements for samples whose structure is changed. The conditions of mechanical stability of unstressed crystalline structures date back a long time [16, 17]. At the microscopic level, the elasticity of the material translates into the ability of the material to return to the minimum energy configuration through the bonding forces of each atom with the surrounding atoms.

RUS is based on the principle that the mechanical resonant response of solids depends strongly on its elastic moduli, shape and density. Resonant (or natural) frequencies of a system can be either measured or calculated by solving equations of motion for the known shape [18].

The reverse is also true; if resonant frequencies of an object are known, it's elastic properties can be determined [18,19]. Energy variation due the deformation ΔU can be write reported to local deformation tensor ε_{ij} [20].

$$\Delta U = \frac{1}{2} C_{ijkl} e_{ij} e_{kl} + \frac{1}{6} C_{ijklmn} e_{ij} e_{kl} e_{mn} + \dots \tag{1}$$

Hooke's generalized law for a solid is

$$\sigma_{ij} = C_{ijkl} \varepsilon_{kl} \tag{2}$$

linearly relates the Cauchy stress σ_{ij} to elastic strain ε_{kl} by elastic stiffness tensor C_{ijkl}.

For the current problem it is assumed that the stress tensor is symmetrical. This implies that $\sigma_{ij} = \sigma_{ji}$, $\varepsilon_{kl} = \varepsilon_{lk}$ and therefore that i and j can be interchanged in equation (2). With "minor symmetry" for 9 components elastic strain and stress require $C_{ijkl} = C_{jikl}$, reducing the number of unique components of the second and fourth rank tensors.

Moreover, the time dependence of the movement can be assumed to be that of a harmonic motion, given by

$$\hat{u}_i(\vec{x}, t) = u_i(\vec{x}) e^{i\omega t} \tag{3}$$

and the fact that the voltage tensor can be written

$$\varepsilon_{kl} = \frac{1}{2} [\hat{u}_{k,l} + \hat{u}_{l,k}] = \frac{1}{2} [u_{k,l} + u_{l,k}] e^{i\omega t} \tag{4}$$

The voltage tensor is also symmetrical. The alternative to representing Hooke's law, using Voigth contraction notation, is

$$\{\sigma\} = [C]\{\varepsilon\} \tag{5}$$

The matrix C can be written as

$$C = \begin{pmatrix} C_{11} & C_{12} & C_{12} & 0 & 0 & 0 \\ C_{12} & C_{11} & C_{12} & 0 & 0 & 0 \\ C_{12} & C_{12} & C_{11} & 0 & 0 & 0 \\ 0 & 0 & 0 & C_{44} & 0 & 0 \\ 0 & 0 & 0 & 0 & C_{44} & 0 \\ 0 & 0 & 0 & 0 & 0 & C_{44} \end{pmatrix} \tag{6}$$

where [21] $C_{11} = \dfrac{E(1-\upsilon)}{(1-\upsilon)(1-2\upsilon)}$; $C_{12} = \dfrac{E\upsilon}{(1-\upsilon)(1-2\upsilon)}$ and $C_{12} = C_{11} - 2C_{44}$.

Using the Voigt approximation, Poisson ratio ν, Young's modulus, shear modulus G are obtained. .
Measurements were made at room temperature using resonant ultrasound spectroscopy (RUS) [22]. The method uses the normal modes of vibration of the solid specimen with known geometry having known crystal symmetry and density so that the elastic tensor can be determined. Determining the resonance frequencies by simulation requires knowledge of the physical properties (size, mass, density) of the specimen. RUS involves knowing the resonant frequencies, obtained experimentally, and based on them de-terminating the elastic constants. The analytical calculation methods do not exist, so an adjustment procedure (computational fitting) is addressed, which, based on an iterative algorithm, matches the resonance frequencies obtained by simulation with those determined experimentally. The elastic constants used in the simulation are left as adjustable parameters and then the iteration can be performed. Thus, through the iteration procedure, generating a multitude of resonant frequencies calculated based on the values entered in the simulator, adjusting the constants, the experimental frequencies match those in the theoretical spectrum. The RUS algorithm consists of two steps, forward and inverse problem. The quality of the determinations is established using RMS error.

$$\sigma_{RMS} = 100 \times \sqrt{\frac{1}{N} \sum_{i=1}^{N} \left(\frac{g_i - f_i}{f_i}\right)^2} \% \tag{7}$$

where $f_i = \omega_i / 2\pi$ is i[th] calculated frequency and g_i is i[th] measured frequency, N is higher number of resonant frequencies involved in optimization, so that to exist sufficient modes of analysis.
For an RMS less than 0.5% it is considered that the elastic constants generated by the computer are the real ones of the sample. The setup and signal processing for RUS method extensively described in [12] were used.
The elastic parameters are mathematically approximated, so that the measurement determines the resonant frequencies of the sample, which constitute input parameters for the calculation algorithm.
Each specimen NMG or NMAG were placed between two identical piezoelectric US transducers, for emission and reception respectively. The samples were fixed between the emission and reception transducers for accomplish the condition of stress-free surface. The frequency bandwidth used for each specimen was adjusted to include a significant number of resonant frequencies (usually 140-320KHz).

3. RESULTS AND DISCUSSIONS

The samples contains a single phase with austenitic type structure, with the grain boundaries being well highlighted having relatively equal sizes, specific to the annealing structure, polygonal and equiaxial [11]. X-ray diffraction indicated that the as casted NMG and NMAG alloys have a cubic Fm3m (L2$_1$) structure, distorted by the presence of the Al, smaller as Ga.
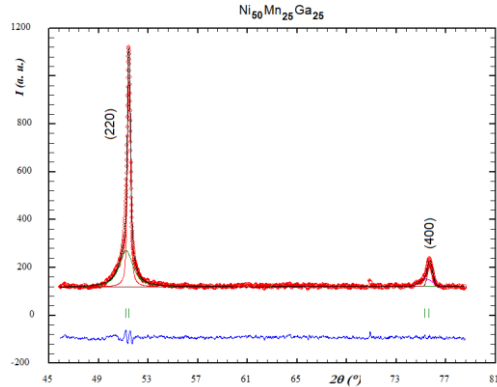
Figure 2: Diffractogram of cast NMG alloy (observed data-black; calculated data-red; difference between the observed and calculated data-blue; Bragg position - green).
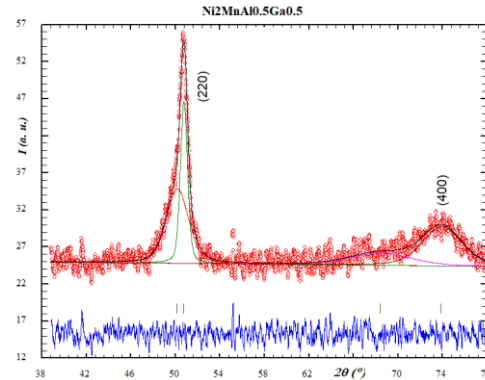
Figure 3: Diffractogram of cast NMAG alloy (observed data-black; calculated data-red; difference between the observed and calculated data-blue; Bragg position - green).

The NMG alloy show that (220) austenite peak is narrow relatively strong figure 2. For NMAG alloy the reflection (220) cubic peak becomes broader and peak (400) increasing. Structure L2$_1$ confirm the austenite phase with the lattice parameter a=5.829A using the powder cell software. The results in Figure 3 suggest that Al entered the structure. From the ingots, cylindrical specimens with dimensions 8x8.3mm of the cubic phase were cut. For this samples the US longitudinal (C$_l$) and transversal (C$_t$) velocities were determined by the pulse-echo method at Tr. From the measured velocities the elastic constants were obtained, the values were mediated for a number of five independent determinations. Using the RUS method, the elastic properties are estimated by comparing the measured resonant frequencies (f^{exp}) with the frequencies provided by the model(f^{calc}). The mass, density and geometry of the specimen are determinant in establishing the frequencies, which allows their adjustment until reaching the best experiment-model match.
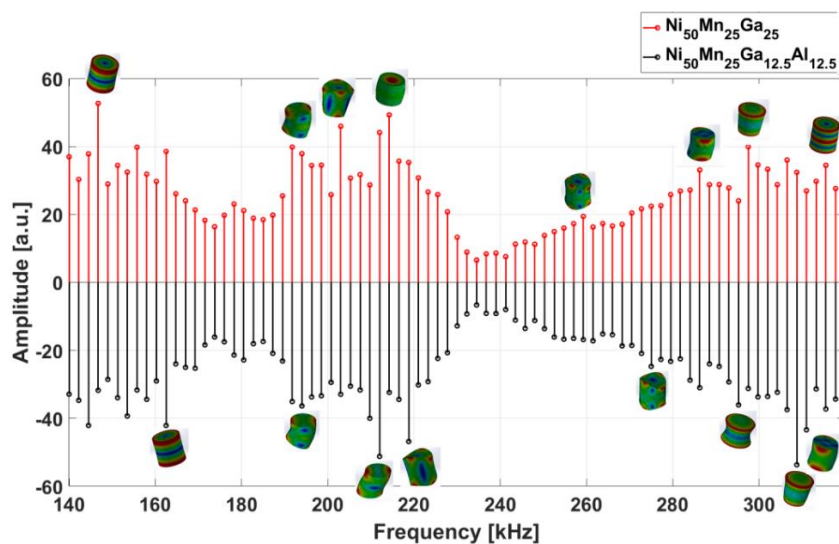
*the color from cubes represent the magnitude of displacement during vibration
** The missing of vibrations as well as the minimal displacements appears in high blue, the maxima in red and the intermediated ones in yellow or green.

Figure 4: A selected interval of the RUS spectrum of Heusler alloys. For representative modes resonant peaks, the modal shape obtained by the RUS the corresponding modal shapes determined within the inversion are normalized to the fundamental torsional frequency.

Resonance occurs when the frequency of US excitation approaches the natural frequency of the sample vibration mode. Recordings were made in a large number of points to cover the entire spectrum of frequencies. The frequency sweep has included a large number of excitation frequencies. According to [23] the modes observed on samples must falls into the following three categories: torsional axisymmetric; extensional and flexural modes (these modes occur in pairs named doublets, with the same resonance frequency). However, frequency ranges that are not covered by resonant frequencies as well as calculated resonant frequency values that do not occur in the spectrum can be observed. The representative modes are obtained by simulation for Poisson coefficients given in Table 1. The modes were visually identified by analyzing the shape of the mode predicted by nodal eigenvectors [24]. Initially, the frequency change analysis has included over 15 modes. For several reasons, it has been established that in the frequency range, 8 modes provide the best information on the samples.

The torsion modes have the maximums at the ends of the diagonals and the lack of vibration displacements along the axis of rotation. The modes were identified by the difference in response to the applied excitation, slight deviations from the cylindrical shape are possible which produces a variation in the resonant frequency of the first ten modes, but which does not influence the interpretation.

Although there are an infinite number of theoretical vibration modes for solids of precise geometric shape, for an efficient and precise determination the inversion of data is used, implying conjugate gradient method minimizing the objective function. The material constants are estimated, according to [25], using a genetic algorithm with ability to find a global minimum with a large and discreet solution space. The cost function is [26]

$$F\left(C_{ij}\right) = \sum_{n=1}^{Nf}\left[w_n \left(\frac{f_n^{exp} - f_n^{num}\left(C_{ij}\right)}{f_n^{exp}} \right)^2 \right] \qquad (8)$$

where f_n^{exp} are the resonant frequencies in the recorded spectrum and f_n^{calc} represent the frequencies calculated for the set of elastic constants, w_n the weighting factor, N_f the number of resonant frequencies.

Since most modes are shear, a number N large enough to comprise several extension modes is chosen. The value of the Poisson's ratio was evaluated at the stationary point of the cost function.

Thus, each determined frequency is correctly associated with the prescribed frequency. This operation is not simple, experimental determinations cannot always go through all the modes expected by simulation, and also the order of their occurrence may differ from those determined experimentally. The optimization problem was numerically solved using Matlab 2020 a. The resonance spectra were traced for cylindrical samples whose properties have been presented in table 1. The frequency answers of the samples that show cubic crystallographic symmetry, have for the shear and flexural mode three groups that give identical results, reason for which only one of each must be taken into study.

The experimental spectra measured in the frequency band limited to 140-320kHz corresponded to a number of 10 modes. The amplitude responses to the resonant frequencies are closely correlated with the sample structure. The eigen frequency intervals show displacements compared to the values obtained theoretically in an acceptable range. It can be observed for eigen resonance frequencies some more pronounced amplitude values, these are related to the properties of the sample, i.e. density and / or crystallographic structure.

First of all, on the homogeneity, there were 3 relatively large changes of frequencies in the spectrum; keeping a small error percentage (0.08) compared to the frequency determined by simulation and RUS. Many higher order modes have similar mode shapes and tend to change in appearance as the frequency increases, making it inadequate to identify the mode in the frequency spectrum.

3. CONCLUSIONS

Heusler alloys, possible candidates for magnetic shape memory alloys, with the chemical structure MNG, have a variety of properties which depend on the chemical composition and crystallographic state. Conventional RUS, allows the determination of the elastic properties of solid materials with a regular geometry. However, the calculation of natural resonance frequencies is limited by the crystallographic structure of the sample. Small anisotropies do not split the fundamental torsion mode for short cylinders (D / L ~ 1), but when associated with dimensional variations they shift the resonant frequency affecting the interpretation of modes. For NMG alloys, an extreme sensitivity to the variation of the Ga component in the structure as well as under the action of a low stress at the RUS frequency in the experiment was observed. It can be assumed that this is related to the behavior of the domain walls. Using data provided by X-ray diffraction and electron microscopy on cubic structures typical of Heusler alloys, it was possible to analyze them by the ultrasound resonance method. RUS spectrogram changes both in amplitude and in phase depending on the properties of the sample, i.e. density and / or crystallographic structure.

REFERENCES

[1] Heusler F., Verhandlungen der Deutschen Physikalischen Gesellschaft 5, 219 (1903).

[2] Planes A., Mañosa L., Moya X., Krenke T., Acet M. and Wassermann E.F., 2007. Magnetocaloric effect in Heusler shape-memory alloys. Journal of Magnetism and Magnetic Materials, 310(2), pp.2767-2769.

[3] de Groot R. A., Mueller F. M., van Engen P. G. and Buschow K. H. J.. New class of materials: Half-metallic ferromagnets. Phys. Rev. Lett., 50:2024–2027, Jun 1983.

[4] Elphick K., Frost W., Samiepour M., Kubota T., Takanashi K., Sukegawa H., Mitani S. and Hirohata A., 2021. Heusler alloys for spintronic devices: review on recent development and future perspectives. Science and Technology of Advanced Materials, 22(1), pp.235-271

[5] Graf T., Felser C., Parkin S.S.P., Simple rules for the understanding of Heusler compounds, Prog. Solid State Chem. 39 (2011) 1-50

[6] Li X.Z., Zhang W.Y., Valloppilly S. and Sellmyer D.J., 2019. New Heusler compounds in Ni-Mn-In and Ni-Mn-Sn alloys. *Scientific reports*, *9*(1), pp.1-7.

[7] Dadda K., Alleg S., Saurina J., Escoda L. and Suñol J.J., 2021. Structure, Microstructure, and Magnetic Properties of Melt Spun Ni50Mn50− xInx Ribbons. *Magnetochemistry*, *7*(5), p.63.

[8] Murray S.J., Marioni M., Allen S.M., O'Handley R.C. and Lograsso T.A., 2000. 6% magnetic-field-induced strain by twin-boundary motion in ferromagnetic Ni–Mn–Ga. *Applied Physics Letters*, *77*(6), pp.886-888.

[9] Buchelnikov V.D., Sokolovskiy V.V., Herper H.C., Ebert H., Gruner M.E., Taskaev S.V., Khovaylo V.V., Hucht A., Dannenberg A., Ogura M. and Akai H., 2010. First-principles and Monte Carlo study of magnetostructural transition and magnetocaloric properties of Ni 2+ x Mn 1− x Ga. *Physical Review B*, *81*(9), p.094411.

[10] Lanska N., Ullakko K. and Lindroos V.K., Composition and temperature dependence of the crystal structure of Ni–Mn–Ga alloys, Journal of Applied Physics, vol. 95, pp. 8074-8078, 2004

[11] Craus M.L., Dobrea V. and Lozovan M., 2008. Martensite-austenite and ferromagnetic-paramagnetic transformations in Ni 2-x A x Mn 1-y B y Ga 1-z C z (A, B= Co; C= Al) Heusler alloys. Revista de Chimie, 59(12), pp.1345-1347.

[12] Savin A., Craus M.L., Turchenko V., Bruma A., Dubos P.A., Malo S., 2015. Monitoring techniques of cerium stabilized zirconia for medical prosthesis. *Applied Sciences*, *5*(4), pp.1665-1682

[13] Soto-Parra D.E., Moya X., Mañosa L., Planes A., Flores-Zuñiga H., Alvarado-Hernandez F., Ochoa-Gamboa R.A., Matutes-Aquino J.A. and Rios-Jara D., 2010. Fe and Co selective substitution in Ni2MnGa: Effect of magnetism on relative phase stability. Philosophical Magazine, 90(20), pp.2771-2792.

[14] Leisure R.G. and Willis F.A., 1997. Resonant ultrasound spectroscopy. Journal of Physics: Condensed Matter, 9(28), p.6001.

[15] Auld B. A. Acoustic fields and waves in solids, 2nd edition, volume 1. Krieger, Malabar, Florida, 1990.

[16] Born M., 1940, April. On the stability of crystal lattices. I. In Mathematical Proceedings of the Cambridge Philosophical Society (Vol. 36, No. 2, pp. 160-172). Cambridge University Press.

[17] Born M., Huang K. and Lax M., 1955. Dynamical theory of crystal lattices. American Journal of Physics, 23(7), pp.474-474.

[18] De Silva C.W. Vibration: fundamentals and practice. CRC Press: Boca Raton, FL, 2000.

[19] Migliori A., Sarrao J., Visscher W.M., Bell T., Lei M., Fisk Z., Leisure R. Resonant ultrasound spectroscopic techniques for measurement of the elastic moduli of solids. Physica B: Condensed Matter 1993, 183, 1, 1-24.

[20] Landau L.D., Lifshitz E.M., Theory of Elasticity, Second ed., Pergamon, 1982.

[21] Lemaitre J, Chaboche J L 1994 Mechanics of solid materials (Cambridge: Cambridge University Press)

[22] Migliori A. and Maynard J.D., 2005. Implementation of a modern resonant ultrasound spectroscopy system for the measurement of the elastic moduli of small solid specimens. Review of scientific instruments, 76(12), p.121301.

[23] Myasnikov DV, Konyashkin AV, Ryabushkin OA 2010 *Tech. Phys. Lett.* **36**(7) 632

[24] Yaoita A, Adachi T and Yamaji A 2005 NDT & E Int. 38(7)554.

[25] Haup Haupt, R.L. and Haupt, S.E., 2004. *Practical genetic algorithms*. John Wiley & Sons

[26] Remillieux M.C., Ulrich T.J., Payan C., Rivière J., Lake C.R. and Le Bas P.Y., 2015. Resonant ultrasound spectroscopy for materials with high damping and samples of arbitrary geometry. Journal of Geophysical Research: Solid Earth, 120(7), pp.4898-4916.